Catal Lett (2009) 130:254–260
DOI 10.1007/s10562-009-9878-1

Effect of Mg Addition on the Physical and Catalytic Properties of Cu/CeO_2 for NO + CO Reduction

Jinfa Chen · Junjiang Zhu · Chongqi Chen · Yingying Zhan · Yanning Cao · Xingyi Lin · Qi Zheng

Received: 22 November 2008 / Accepted: 24 January 2009 / Published online: 5 February 2009

Abstract Copper catalysts supported on magnesia promoted ceria are synthesized and used for NO reduction by CO. The supports and the subsequent Cu catalysts are prepared by citric acid sol–gel and impregnation methods, respectively. The results of N_2-physisorption, XRD, EPR and TPR measurements indicate that the Mg addition promotes not only the dispersion of CuO, but also the formation of Cu–O–Ce solid solution. The highest amount of Cu–O–Ce solid solution is found in catalyst modified with 5 wt.% MgO. Based on the catalytic performance, two active sites for the reduction NO by CO are proposed: copper matrix and Cu–O–Ce solid solution. The former does not require the involvement of oxygen vacancy and is more active at low temperature range ($T < 200$ °C), while the latter shows higher NO conversion at temperature above 200 °C, due to the easy regeneration of oxygen vacancy. Also, it is found that the NO conversion over copper matrix is suppressed, while that over Cu–O–Ce solid solution is stimulated in high CO concentration.

Keywords NO reduction by CO · Ceria · Magnesia doped ceria · Copper · Active site

J. Chen · C. Chen · Y. Zhan · Y. Cao · X. Lin · Q. Zheng (✉)
National Engineering Research Center of Chemical Fertilizer Catalyst, Fuzhou University, Gongye Road 523, Fuzhou 350002, Fujian, China
e-mail: zhengqi@fzu.edu.cn

J. Zhu
Laboratory of Catalysis and Materials Department of Chemical Engineering Faculty of Engineering, University of Porto, 4200-465 Porto, Portugal

1 Introduction

Nitrogen oxide (NO) is one of the major air pollutants and leads to acid rain and ozone depletion, so the study of catalytic reduction of nitrogen oxide has drawn much attention, recently. Particularly, a great deal of efforts has been made on the reduction of nitric oxide (NO) by carbon monoxide (CO), as these two gases are co-existed pollutants in automobile exhaust. Today, the most popular catalyst used for purifying automobile exhaust are three-way catalysts (TWCs), which, however, consist of precious metals that are rather expensive. Hence, many efforts on exploring efficient base metal catalyst for exhaust purification have been attempted in the last decades, to lower the cost of the catalyst.

Copper based catalysts are promising candidate for the catalytic reduction of NO by CO. It has been reported that Cu-based catalysts, such as Cu-exchanged zeolites [1], Cu-containing perovskite catalysts [2–4], and copper oxides supported on metal oxides [5–7] etc., exhibit good catalytic activity for NO abatement reactions. Among them, Cu/CeO_2 and $Ce_{1-x}Cu_xO_2$ have been received great attention, due to the unique redox behavior of CeO_2 and the special interaction between copper and ceria [8–10]. Compared with pure ceria, the doped one possesses higher oxygen storage capacity (OSC) and better thermal stability. For example, it has been reported that the incorporation of Zr^{4+} to CeO_2 forms $Ce_xZr_{1-x}O_2$ solid solution, leading to the decrease of cell volume, lowering the activation energy for oxide-ion diffusion and increasing the OSC and thermal stability [11, 12]. Similar phenomenon was also observed by Hf^{4+} doping [13]. The doping of ceria with trivalent metal ion is also widely investigated since the replacement of tetravalent cerium by a metal with low oxidation state, according to the principle of electroneutrality, could

provide the opportunity of producing oxygen vacancies, which have been proved to play an important role in CO oxidation [14, 15] and NO reduction [16–20]. Whereas, the replacement of tetravalent cerium by a bivalent metal is still in its infancy, it thus becomes the objective of this work.

Magnesia has been reported to be a promoter for the dispersion of metal on $MgO–CeO_2$ supports [21] and for the creation of oxygen vacancy through the formation of $Ce_{1-x}Mg_xO_2$ [22], both of which would produce positive effect on the catalytic performance of Cu/CeO_2 catalyst. Therefore, here we also choose MgO as an additive, to study its effect on the catalytic performance of Cu/CeO_2 for NO + CO reaction. TPR, XRD and EPR measurements were employed to investigate the difference in ceria and Mg-doped ceria and, to disclose the copper oxide species loaded on them. Based on the catalytic activity tested under different reaction conditions, it is considered that both metallic copper and Cu–O–Ce solid solution are active for NO + CO reaction. Moreover, it is found that the catalytic activity of copper matrix is suppressed, while that of Cu–O–Ce solid solution is stimulated with the increase of CO concentration.

2 Experimental

2.1 Catalyst Preparation

All chemical reagents used in this work are A.R. grade. Mg-doped ceria (Mg contents: 0, 5, 10 wt.%) were prepared by citric acid sol–gel method. In a typical procedure, a calculated amount of cerium (III) nitrate hexahydrate, magnesium nitrate hexahydrate and citric acid monohydrate (50% in excess of stoichiometry) were mixed together and dissolved in an appropriate amount of distilled water. The solution was then heated to 70 °C and kept for 1.5 h with continuous stirring. The resulting gel was subsequently dried in air at 150 °C for 3 h and finally calcined at 600 °C for 6 h. The obtained supports were donated as CeO_2, CM5 and CM10, corresponding to 0, 5, 10 wt.% Mg contents, respectively.

Copper catalysts (loading: 5 wt.%) were prepared by a modified impregnation method: first, adding the support to $Cu(NO_3)_2 \cdot 3H_2O$ aqueous solution, the slurry was then stirred slowly at 60 °C for 1 h, dried at 100 °C for 8 h and finally calcined at 600 °C for 6 h. Based on the supports, the prepared catalysts were named as Cu/CeO_2, Cu/CM5 and Cu/CM10, respectively.

2.2 Characterizations

Temperature programmed reduction (TPR) was performed on an AutoChem 2910 instrument. The sample (50 mg) was first treated in Ar stream at 200 °C for 1 h and cooled to room temperature in the same atmosphere, then swept with $10\%H_2/Ar$ until the baseline on the recorder unchanged. The sample was finally heated in $10\%H_2/Ar$ from room temperature to 400 °C for copper catalysts and to 850 °C for supports at a rate of 10 °C/min.

Powder XRD patterns of the as-synthesized samples were recorded by a PANalytical X' pert Pro diffractometer with an X'Celerator detector, operating at 40 kV and 40 mA and using Co Kα radiation ($\lambda =$ 0.17,902 nm).

BET surface area and pore volume were measured by a Micromeritics ASAP 2020 physical adsorption analyzer at −196 °C using nitrogen as adsorbate. Prior to each analysis, the sample was degassed at 200 °C for 4 h.

Electronic paramagnetic resonance (EPR) spectra were obtained by a Brucker EMX-10/12 spectrometer at 97 K, with the klystron frequency of 9.6 GHz and the magnetic field modulation of 100 kHz.

2.3 Catalytic Activity Measurements

NO + CO reaction was tested in a quartz glass reactor, equipped with a temperature program controller. The reaction temperature was raised from 150 to 400 °C with an interval of 50 °C. Two kinds of feed gas were used to evaluate the catalytic performance of the Cu catalysts, feed gas I: 5,000 ppm NO and 5,000 ppm CO and feed gas II: 6,000 ppm CO and 4,800 ppm NO, with a total flow rate of 36 mL/min. The sample weight is 70 mg for each test. Prior to each measurement, the catalyst was firstly purged with pure helium at 550 °C for 1 h and subsequently reduced by 1% CO/He at 300 °C for 1 h. The product was monitored by GC (Agilent 6820) equipped with a thermal conduction detector (TCD). Two packed columns were adopted to separate the products: Porapak Q column for separating N_2O and CO_2, and 5A molecular sieve column for separating N_2, NO and CO.

CO conversion, NO conversion and N_2 selectivity were calculated using the following formulas:

$$\%[CO]_{conv.} = \frac{[CO]_{inlet} - [CO]_{outlet}}{[CO]_{inlet}} \times 100$$

$$\%[NO]_{conv.} = \frac{[NO]_{inlet} - [NO]_{outlet}}{[NO]_{inlet}} \times 100$$

$$\%[N2]_{sel.} = \frac{2[N2]_{outlet}}{[NO]_{inlet} - [NO]_{outlet}} \times 100$$

Where $[CO]_{inlet}$, $[NO]_{inlet}$ and $[CO]_{outlet}$, $[NO]_{outlet}$ are the initial and final concentration of CO and NO, respectively; $[N_2]_{outlet}$ is the N_2 concentration in the product.

3 Results and Discussion

3.1 XRD Characterization

The X-ray diffraction patterns of the as-prepared supports and catalysts are shown in Fig. 1. For all catalysts doping with MgO, the diffraction peaks indexed to MgO are hardly observed, suggesting that MgO is well dispersed and/or incorporates into the lattice of ceria. Furthermore, it is found that the cell parameters (see in Table 1) of CeO_2 (5.406 Å) are decreased after the MgO doping (5.400 Å), which also indicate that smaller Mg^{2+} ions may insert into the lattice of CeO_2, forming nonequilibrium solid solution $Ce_{1-x}Mg_xO_2$. Besides, the decrease of the crystallite size (i.e., CeO_2 > CM5 > CM10) indicates that the addition of MgO could suppress the agglomeration of CeO_2 particles. After loading of Cu, it is interesting to find that the intensity of diffraction peaks indexed to CuO (marked with '▼') weakens and broadens with the increase of Mg content (Fig. 1d–f), which implies the improvement of CuO dispersion after doping with MgO. Meanwhile, no obvious change in the cell parameter is observed, but we do not exclude the possibility of formation of Cu–O–Ce solid solution, since Cu–O–Ce solid solution presents on the surface of ceria lattice can not be detected by XRD [22–26]. Therefore, further investigations are performed to study whether the Cu–O–Ce solid solution is formed.

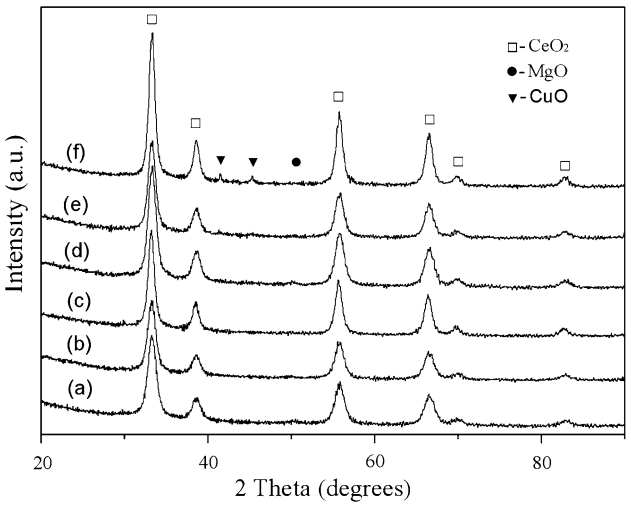

Fig. 1 X-ray diffraction patterns of the supports and catalysts. (*a*) CM10; (*b*) CM5; (*c*) CeO_2; (*d*) Cu/CM10; (*e*) Cu/CM5; (*f*) Cu/CeO_2

Table 1 Physical property of the supports and catalysts

Sample	S_{BET} (m^2/g)	Pore volume (mL/g)	Crystallite size[a] (nm)	Cell parameter[a] (Å)
CeO_2	52	0.099	12.3	5.406
CM5	33	0.073	9.8	5.400
CM10	32	0.060	9.4	5.400
Cu/CeO_2	43	0.089	12.9	5.406
Cu/CM5	31	0.070	10.1	5.401
Cu/CM10	45	0.082	9.9	5.401

[a] Data are calculated by a self-program of the XRD diffractometer

3.2 N_2 Physisoption Measurement

The results in Table 1 show that for CeO_2, CM5 and CM10, the BET surface area and pore volume, as well as the particle size of CeO_2, decrease with the increase of MgO content. It is worthwhile to point out that CeO_2 with bigger particle size shows larger BET surface area, which is contrary to the general knowledge, a possible reason is that some pores of CeO_2 were blocked by small MgO crystallites when MgO was added, and thus leading to the decrease of BET surface area. This can be confirmed by the fact that the pore volume of CeO_2 (0.099 mL/g) is larger than that of CM5 (0.073 mL/g) and CM10 (0.060 mL/g), similar phenomenon was also observed by Sato et al. [27]. After loading of Cu, the changes of BET surface area are so different: for pure CeO_2, the BET surface area increases greatly (from 52 to 43 m^2/g); for CM5, the variation is slight (from 33 to 31 m^2/g); while for CM10, the BET surface area is even increased (from 32 to 45 m^2/g). This could be explained by the reconstruction of MgO during impregnation and calcination processes. That is, the MgO crystal in the pore of CeO_2 would dissolve in the impregnation process when $Cu(NO_3)_2 \cdot 3H_2O$ solution was present, cleaning the CeO_2 pore and hence increasing the BET surface area, as described elsewhere [28].

3.3 EPR Spectra

Figure 2 shows the EPR spectra of Cu/CeO_2, Cu/CM5 and Cu/CM10. The EPR spectra exhibit four copper signals: A_1, A_2, B, and K. Signal K, showing $g_\perp = 2.040$ and unresolved parallel component, is ascribed to the copper(II) ion pairs in ceria, i.e., the substitution of two Cu^{2+} ions for two neighboring Ce^{4+} ions in the lattice with the smallest distance (3.811 Å) [29]. This substitution only occurs on the surface and does not destroy the matrix structure of CeO_2. Compared with Cu/CeO_2, Cu/CM5 shows stronger intensity in signal K, indicating that the addition of MgO promotes the substitution of Cu^{2+} for Ce^{4+}. However, when more MgO is introduced (i.e., Cu/CM10), the intensity of signal K decreases (Fig. 2c). The reason is similar to that observed in Signal A_1, as discussed below.

Signal A_1, which is contributed by isolated Cu^{2+} in octahedral sites of ceria with a tetragonal distortion [30–33], exhibits four-line hyperfine splittings and shows $g_\parallel = 2.345$, $A_\parallel = 125$ G for Cu/CeO_2, $g_\parallel = 2.331$, $A_\parallel = 153$ G for Cu/CM5 and $g_\parallel = 2.327$, $A_\parallel = 153$ G for

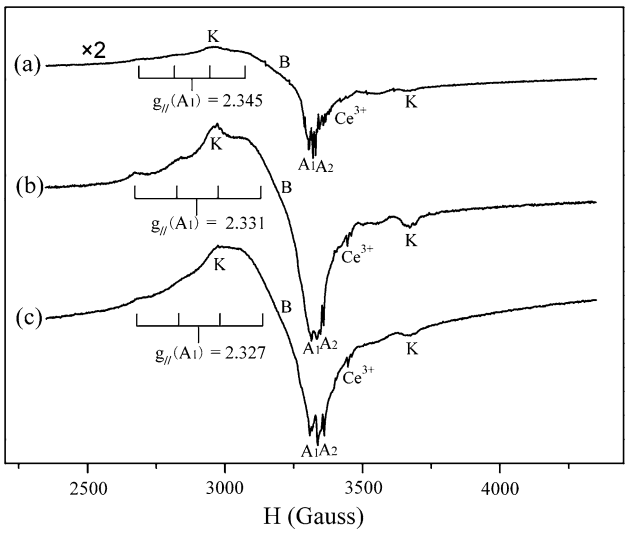

Fig. 2 EPR spectra of the catalysts: (*a*) Cu/CeO_2, (*b*) Cu/CM5 (*c*) Cu/CM10

Cu/CM10. Compared with those of Cu/CeO_2, the lower $g_{||}$ values and the higher $A_{||}$ values of Cu/CM5 and Cu/CM10 suggest that the tetragonal distortion increases after MgO is introduced [34]. Also, it is found that the intensity increases with the increase of MgO content at the beginning (i.e., Cu/CM5), but then decreases with further increase of MgO content (i.e., Cu/CM10). The reason might be that for Cu/CM10, large part of ceria surface is previously covered by MgO, which subsequently occupies the octahedral sites of ceria [the ionic radius of Mg^{2+} (0.072 nm) is similar with Cu^{2+} (0.073 nm)], resulting in less octahedral sites available for Cu^{2+}. In addition, according to the results of literatures [35, 36] these Cu^{2+} monomeric ions are the precursors for the copper(II) ion pairs in ceria. Therefore, in our case, the catalyst with higher intensity of signal A_1 also shows higher intensity of signal K.

Signal A_2 is attributed to isolated Cu^{2+} localized in surface substitution sites of ceria [33]. It has been reported that ionic mobility stimulated by anion vacancies or high temperature could promote the substitution of Cu^{2+} for Ce^{4+} [37]. Herein, due to the limitation of oxygen vacancies in the pure ceria and the relatively low calcination temperature, only few copper ions could incorporate into the ceria lattice in Cu/CeO_2 system. While for samples doped with MgO, more oxygen vacancies are created due to the formation of nonequilibrium solid solution $Ce_{1-x}Mg_xO_2$ and therefore, more Ce^{4+} could be substituted by Cu^{2+} ions. However, it is hard to determine the $g_{\perp}$ value for both signals A_1 and A_2 due to the overlapping of the perpendicular components of them.

Signal B, showing extremes at $g \approx 2.22$ and $g \approx 2.04$, is also ascribed to Cu^{2+} ions, its larger linewidth (leading to unresolved hyperfine splitting) is attributed to the dipolar broadening effects caused by mutual interactions between paramagnetic Cu^{2+} ions of an oxide type [34]. Since antiferromagnetic couplings between Cu^{2+} ions in well-crystallized CuO phases produce EPR-silent species [38, 39], the Cu^{2+} ions yielding signal B here thus could be considered as belonging to small copper oxide clusters. Hence, the stronger intensity of signal B observed in Cu/CM5 and Cu/CM10 (vs. Cu/CeO_2) suggests that there are more small copper oxide clusters, or in other word, a better dispersion of CuO in Cu/CM5 and Cu/CM10.

Also, a signal contributed by Ce^{3+} ($g = 1.960$) is observed in the samples and its intensity in Cu/CM5 and Cu/CM10 is stronger than that in Cu/CeO_2. The reason might be that there exists Mg^{2+} ions and more Cu^{2+} ions could enter the CeO_2 lattice (see above) in the latter two samples. As a result, more Ce^{3+} ions and oxygen vacancy could be produced in them, resulting in the stronger intensity of signal at $g = 1.960$.

3.4 TPR Results

H_2-TPR measurements are adopted to characterize the reduction properties of the as-prepared samples, and the results are shown in Fig. 3. From Fig. 3a, we can see that

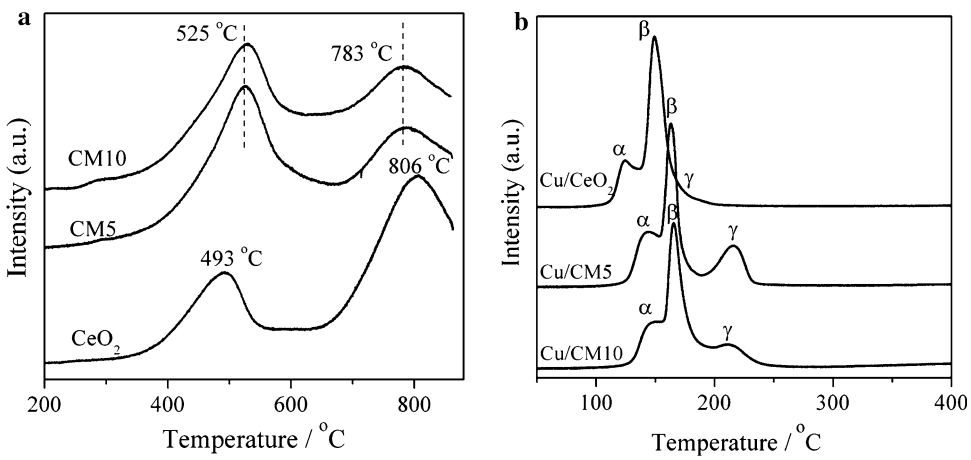

Fig. 3 TPR profiles of the samples: **a** supports; **b** copper catalysts

there are two reduction peaks for CeO_2 support in the temperature range of 200–870 °C, which are ascribed to the reduction of surface and bulk oxygen of CeO_2 [40], respectively. After MgO is added, the reduction peak centered at about 493 °C shifts to 525 °C, accompanying with the increase of peak area. Based on the XRD results, it is known that due to the formation of the nonequilibrium solid solution $Ce_{1-x}Mg_xO_2$, more oxygen vacancies are produced (Mg^{2+} vs. Ce^{4+}), so some of bulk oxygen in CeO_2 are activated and transferred onto surface oxygen, thus increasing the peak area increases and postponing the appearance of peak maximum from 493 to 525 °C.

TPR profiles of the Cu catalysts are shown in Fig. 3b and the corresponding hydrogen consumption values are summarized in Table 2. All the catalysts show three reduction peaks (denoted as peak α, β and γ, respectively). The peak α and β can be ascribed to different copper-oxide entities dispersed on the surface of ceria [41]. The peak γ can be assigned to the reduction of copper ions in ceria lattice, since copper ions in ceria lattice are more difficult to be reduced [42, 43]. It can be seen that the intensity of peak γ follows the sequence of Cu/CM5 > Cu/CM10 > Cu/CeO_2, which is in accordance with the intensity variation of signals K and A_1 in EPR spectra (see Fig. 2). For all the three Cu catalysts, the measured hydrogen consumption value is higher than that required for the quantitative reduction of CuO to Cu (about 781 $\mu mol/g_{cat}$), indicating that some of ceria participate in the reduction process. Moreover, by comparing with the reduction temperature of pure CeO_2 and the Cu catalysts, it can be seen that the former begins at ~300 °C, while the latter ends at ~250 °C, suggesting that the introduction of copper oxide significantly changes the redox property of ceria. The hydrogen consumption value of the Cu catalysts is in sequence of Cu/CM5 > Cu/CM10 > Cu/CeO_2. This is in the same order as the amount of copper ions being incorporated into ceria lattice (Sec. 3).

Table 2 Hydrogen consumption value of the three copper catalysts in H_2-TPR experiment

Catalyst	H_2 consumption ($\mu mol/g_{cat}$)			Total amount ($\mu mol/g_{cat}$)
	α (°C)	β (°C)	γ (°C)	
Cu/CeO_2	160 (125)	741 (150)	39 (177)	940
Cu/CM5	205 (140)	636 (162)	232 (214)	1,074
Cu/CM10	192 (142)	633 (165)	165 (212)	990

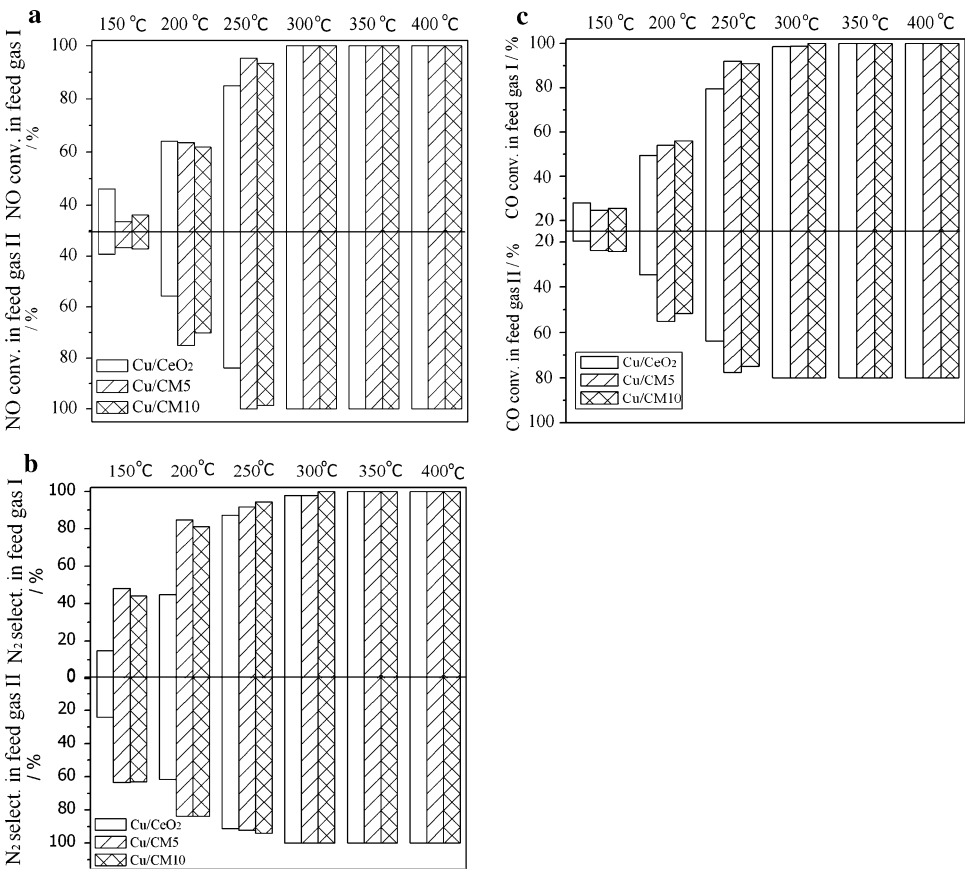

Fig. 4 Activity of the three copper catalysts for **a** NO conversion; **b** N_2 selectivity and **c** CO conversion

3.5 Catalytic Performance

NO + CO reaction is adopted to evaluate the catalytic performance of the catalysts after pretreatment, and the results are shown in Fig. 4. The NO conversion of Cu/CeO_2 is higher than that of Cu/CM5 and Cu/CM10 at low temperature in both feed gas I and II atmosphere, e.g., at 150 °C and 200 °C in feed gas I and at 150 °C in feed gas II. While in high temperature ranges (T > 200 °C), Cu/CeO_2 shows the lowest and Cu/CM5 shows the highest NO conversion. Also, it is found that for Cu/CeO_2, the NO conversion in feed gas I is higher than that in feed gas II, while for the MgO doped catalysts (i.e., Cu/CM5 and Cu/CM10), the NO conversion in feed gas I is lower than that in feed gas II.

The above results indicate that the active sites of Cu/CeO_2 and Mg-doped catalysts for NO + CO reaction is different and their catalytic performances greatly depend on the gas components and reaction temperature. For Cu/CeO_2, as concluded from TPR and EPR measurements, only few copper ions enter the ceria lattice and most of them are dispersed on the surface of ceria. While for Cu/CM5 and Cu/CM10, more Cu^{2+} ions could enter the ceria lattice forming Cu–O–Ce solid solution, and substitution of Cu^{2+} for Ce^{4+} in CeO_2 lattice leads to creation of oxygen vacancies around Cu^{2+}–O–Ce^{4+} on the surface of CeO_2 [44]. It has been reported that oxygen vacancy in ceria plays an important role and acts as the site for NO dissociation in the reaction of NO removal [16–20], and hence the regeneration of oxygen vacancy would be a key process for Cu–O–Ce solid solution maintaining its catalytic activity in NO + CO reaction, and the previous reduction with CO before reaction may result in the creation of more oxygen vacancies around copper sites. Moreover, from the results of TPR characterization, it can be found that the copper ions in ceria lattice require higher reduction temperature than the copper oxide dispersed on the surface of ceria. Correlating these results to the catalytic performance of the as-prepared catalysts, we can conclude that the catalytic activity of Cu/CeO_2 mainly arises from copper matrix, which shows lower NO reduction activity in higher CO concentration, resulting in the better catalytic activity of Cu/CeO_2 in low temperature range; with the increase of reaction temperature, the regeneration of oxygen vacancy turns to be easier and hence higher catalytic activity could be obtained due to more Cu–O–Ce solid solution is formed, as a result, the NO conversion of Cu/CM5 and Cu/CM10 is higher than that of Cu/CeO_2 in higher temperature range, and the active site shows higher NO conversion in higher CO concentration which is different from copper matrix.

When concerning the BET surface area of Cu/CM10 (45 m^2/g) that is higher than that of Cu/CM5 (31 m^2/g), however, the NO conversion of the former is slightly lower than that of the latter one in moderate temperature range, the reason may be ascribed to the less amount of Cu–O–Ce solid solution formed in Cu/CM10.

As for the N_2 selectivity, the results obtained from the two MgO promoted catalysts are always higher than that from Cu/CeO_2, either in feed gas I or in feed gas II, indicating that the formation of copper-ceria solid solution is favor to N_2 selectivity.

4 Conclusion

The addition of 5 wt.% MgO to Cu/CeO_2 system significantly improves the copper dispersion and the amount of Cu^{2+} ions being incorporated into the ceria lattice. Further addition of MgO (10 wt.%) leads to the increase in the BET surface area of Cu/CeO_2, but the decrease in the amount of Cu^{2+} in ceria. There are two active sites, i.e., Cu–O–Ce solid solution and copper matrix, in the catalysts, the former is active in high CO concentration and at moderate temperature (e.g., 200 and 250 °C), while the latter acts mainly at low temperature range and its catalytic activity decreases with the increase of CO concentration. Also, it is found that the formation of copper-ceria solid solution is favor to N_2 selectivity.

Acknowledgments The authors gratefully acknowledge the financial support from the National Natural Science Foundation of China (20771025), the Nature Science Foundation of Fujian Province of China (2007J0221) and the Education Department of Fujian province of China (JB06050).

References

1. Panayotov D, Dimitrov L, Khristova M, Petrov L, Mehandjiev D (1995) Appl Catal B Environ 6:61
2. Zhu J, Zhao Z, Xiao D, Li J, Yang X, Wu Y (2005) J Mol Catal A 238:35
3. Zhang R, Villanueva A, Alamdari H, Kaliaguine S (2006) J Mol Catal A 258:22
4. Mizuno N, Yamamoto M, Tanaka M, Misono M (1991) J Catal 132:560
5. Fernández-García M, Gómez Rebollo E, Guerrero Ruiz A, Conesa JC, Soria J (1997) J Catal 172:146
6. Chien CC, Shi JZ, Huang TJ (1997) Ind Eng Chem Res 36:1544
7. Jiang X, Ding G, Lou L, Chen Y, Zheng X (2004) J Mol Catal A 218:187
8. Bera P, Aruna ST, Patil KC, Hegde MS (1999) J Catal 186:36
9. Wen B, He M (2002) Appl Catal B Environ 37:75
10. Hu Y, Dong L, Shen M, Liu D, Wang J, Ding W, Chen Y (2001) Appl Catal B Environ 31:61
11. Ozawa M, Matuda K, Suzuki S (2000) J Alloys Compd 56:303
12. Reddy BM, Khan A, Lakshmanan P, Aouine M, Loridant S, Volta JC (2005) J Phys Chem B 109:3355
13. Reddy BM, Bharali P, Saikia P, Khan A, Loridant S, Muhler M, Grünert W (2007) J Phys Chem C 111:1878
14. Park JW, Jeong JH, Yoon WL, Jung H, Lee HT, Lee DK, Park YK, Rhee YW (2004) Applied Catalysis A 274:25

15. Wang JB, Tsai DH, Huang TJ (2002) J Catal 208:370
16. Ranga Rao G, Fornasiero P, Di Monte R, Kašpar J, Vlaic G, Balducci G, Meriani S, Gubitosa G, Cremona A, Graziani M (1996) J Catal 162:1
17. Fornasiero P, Ranga Rao G, Kašpar J, L'Erario F, Graziani M (1998) J Catal 175:269
18. Yang Z, Woo TK, Hermansson K (2006) Surf Sci 600:4953
19. Roy S, Hegde MS (2008) Catal Commun 9:811
20. Roy S, Marimuthu A, Hegde MS, Madras G (2008) Catal Commun 9:101
21. Costa CN, Efstathiou AM (2007) Appl Catal B Environ 72:240
22. Hocevar S, Krasovec UO, Orel B, Arico AS, Kim H (2000) Appl Catal B Environ. 28:113
23. Aboukais A, Bennani A, Aissi CF, Wrobel G, Guelton M (1992) J Chem Soc Faraday Trans 88:1321
24. Liu W, Flytzani-Stephanopoulos M (1995) J Catal 153:304–332 (parts I and II)
25. Tschöpe A, Liu W, Flytzani-Stephanopoulos M, Ying JY (1995) J Catal 157:42
26. Ying JY, Tschöpe A, Levin D (1995) Nanostruct Mater 6:237
27. Sato S, Koizumi K, Nozaki F (1998) J Catal 178:264
28. Chen J, Zhu J, Zhan Y, Lin X, Cai G, Wei K, Zheng Q, Submitted
29. Aboukaïs A, Bennani A, Lamonier-Dulongpont C, Abi-Aad E, Wrbel G (1996) Colloid Surface A 115:171
30. Crusson-Blouet E, Aboukais A, Mssi FC, Guelton M (1992) Chem Mater 4:1129
31. Scholz G, Lück R, Stöer R, Lunk HJ, Ritschl F (1991) J Chem Soc Faraday Trans 87:717
32. Clementz DM, Pinnavia TJ, Mortla MM (1973) J Phys Chem 77:196
33. Aboukais A, Bennani A, Aissi CF, Guelton M, Vedrinef JC (1992) Chem Mater 4:977
34. Martínez-Arias A, Fernández-García M, Soria J, Conesa JC (1999) J Catal 182:367
35. Aboukais A, Bennain A, Aissi CF, Wrobel G, Guelton M, Vedrine J (1992) J Chem Soc Faraday Trans 88:615
36. Wagner GR, Schumacher RT, Friedberg SA (1966) Phys Rev 150:226
37. Sofia J, Conesa JC, Martinez-Arias A, Coronado JM (1993) Solid State Ionics 63–65:755
38. Mehran F, Barnes SE, Chandrashekhar GV, McGuire TR, Shafer MW (1988) Solid State Commun 67:1187
39. Kulyova SP, Lunina EV, Lunin VV, Kostyuk BG, Muravyova GP, Kharlanov AN (2001) Chem Mater 13:1491
40. Yao HC, Yu Yao YF (1984) J Catal 86:254
41. Liu Z, Zhou R, Zheng X (2007) J Mol Catal A Chem 267:137
42. Wang X, Rodriguez JA, Hanson JC, Gamarra D, Martínez-Arias A, Fernández-García M (2005) J Phys Chem B 109:19595
43. Luo MF, Song YP, Lu JQ, Wang XY, Pu ZY (2007) J Phys Chem C 111:12686
44. Bera P, Priolkar KR, Sarode PR, Hegde MS, Emura S, Kumashiro R, Lalla NP (2002) Chem Mater 14:3591